ChemComm

COMMUNICATION

View Article Online
View Journal | View Issue

Cite this: *Chem. Commun.*, 2015, 51, 4451

Received 12th December 2014,
Accepted 4th February 2015

DOI: 10.1039/c4cc09926e

www.rsc.org/chemcomm

Anchoring AgBr nanoparticles on nitrogen-doped graphene for enhancement of electrochemiluminescence and radical stability†

Ding Jiang,‡[a] Xiaojiao Du,‡[b] Qian Liu,[b] Nan Hao,[b] Jing Qian,[b] Liming Dai,[b] Hanping Mao[b] and Kun Wang*[b]

AgBr nanoparticles anchored nitrogen-doped graphene nanocomposites were designed to obtain enhanced electrochemiluminescence intensity and better stability, and further applied in electrochemiluminescence detection for the first time.

Electrochemiluminescence (ECL) is the optical emission from the excited states of an ECL luminophore produced at an electrode surface *via* electrochemical high-energy electron transfer reaction, which has attracted growing interest owing to its good analytical performance.[1] Previous reports have demonstrated that both the ECL efficiency[2] and stability[3] of luminophores are the most important criteria when evaluating the performance of light-emitting materials. In the existing mature ECL systems, Ru complexes,[4] luminols,[5] gold nanoclusters,[6] and diverse semiconductors have been widely used as ECL luminophores for fabricating sensing platforms in practical applications.[7] Among them, growing attention in ECL studies of semiconductor nanoparticles (NPs) has emerged because of the unique electrochemical and optical properties of these nanomaterials in recent years.[3] It is still one of the key subjects in the ECL research to identify innovative, stable, and highly efficient ECL luminophores.[8]

As an attractive small bandgap semiconductor, silver bromide nanoparticles (AgBr NPs) have been extensively researched due to its unique light-sensitivity and suitable band potentials.[9] The well documented photoluminescence (PL) spectra and ultraviolet-visible (UV-vis) absorption provide information about the band gap of this semiconductor.[10,11] Therefore, with the small band gap of 2.6 eV, AgBr NPs could be used as an emitting material in light-emitting diodes and display devices.[8,11] It is also possible to be used in the ECL system. However, pure AgBr NPs are unstable under light irradiation since their photogenerated electrons are easily captured by Ag^+, resulting in the instability of the signal, which greatly restricts their further application in the analytical field.[9a,12a]

Coupling AgBr NPs with other appropriate nanosized materials, especially carbon-based materials, is an effective strategy to improve the stability of AgBr NPs and extend their potential applications. Besides, through surface functional modification and the introduction of nanomaterials in ECL systems have been employed to obtain an amplified ECL signal.[12b] Meanwhile, the heteroatom nitrogen can be doped into the graphene carbon lattice to effectively tailor the properties of pristine graphene.[13a] Owing to apparent advantages of N-doping, nitrogen-doped graphene (NG) composite structures can be utilized for facile synthesis of robust composite structures using various functional materials.[13b]

Herein, AgBr NPs anchored nitrogen-doped graphene (AgBr–NG) nanocomposites have been successfully prepared by the water bath method and employed in ECL detection for the first time to overcome the shortcomings mentioned above. The detailed synthesis process is illustrated in the ESI.† Further, the cathodic ECL emission with AgBr NPs as luminophores is observed for the first time. The ECL signal of the AgBr–NG nanocomposites at the glass carbon electrode (GCE) were explored using $K_2S_2O_8$ as the coreactant. It is confirmed that AgBr–NG nanocomposites result in a significantly enhanced and stable ECL emission. Their preliminary application in the determination of heavy metal ions, Pb^{2+}, is also demonstrated, suggesting that AgBr–NG nanocomposites can be promising candidates for the ECL analysis.

The X-ray diffraction (XRD) patterns of the resultant AgBr NPs and AgBr–NG nanocomposites were performed to analyze the phase structure. As shown in Fig. 1A, the XRD patterns of AgBr NPs and AgBr–NG nanocomposites displayed similar diffraction peaks (2θ) at 26.6° (111), 30.8° (200), 44.2° (220), 52.3° (311), 54.9° (222), 65.3° (400), and 74.2° (311), which were ascribed to the diffractions of crystalline AgBr (JCPDS file: 06-0438).[10,11]

[a] *School of Food and Biological Engineering, Jiangsu University, Zhenjiang, 212013, P. R. China*
[b] *Key Laboratory of Modern Agriculture Equipment and Technology, School of Chemistry and Chemical Engineering, Jiangsu University, Zhenjiang, 212013, P. R. China. E-mail: wangkun@ujs.edu.cn; Tel: +86 511 88791800*

† Electronic supplementary information (ESI) available. See DOI: 10.1039/c4cc09926e

‡ These authors contributed equally to this work.

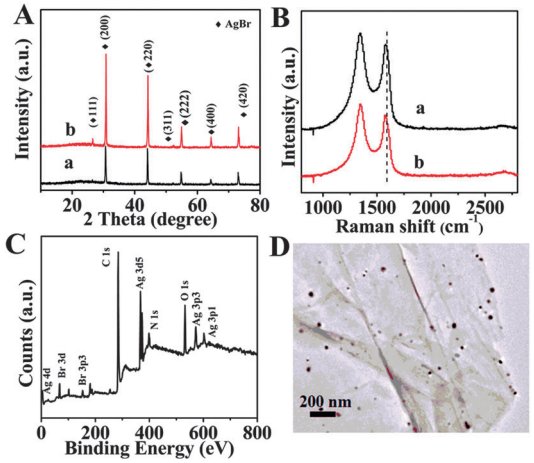

Fig. 1 (A) XRD patterns of AgBr NPs (a) and AgBr–NG nanocomposites (b); (B) Raman spectra of powdery NG (a) and AgBr–NG nanocomposites (b); (C) the XPS spectrum and (D) typical TEM images of the synthesized AgBr–NG nanocomposites.

The existence of NG can be determined by the following Raman spectra (Fig. 1B). Two characteristic peaks of the graphitic material, namely D and G bands, were observed in AgBr–NG nanocomposites and at around 1350 cm^{-1} and 1590 cm^{-1}, respectively, which resembled those of AgBr–graphene nanocomposites (Fig. 1B, curve a).[11] To further verify the hybridization structure of AgBr–NG nanocomposites, the surface elemental compositions of the as-prepared nanocomposites were characterized by X-ray photoelectron spectroscopy (XPS). The XPS scan spectra of AgBr–NG nanocomposites exhibited distinct Ag 3d, Br 3d, C 1s, N 1s and O 1s peaks (Fig. 1C), revealing the predominant presence of Ag, Br, C, N and O elements. The high-resolution XPS spectrum of Ag 3d, Br 3d, C 1s, and N 1s was shown in Fig. S1 (ESI†). The morphological observations were carried out using transmission electron microscopy (TEM). As presented in Fig. 1D, it is obvious that both the outline of NG and AgBr NPs could be clearly observed and the two-dimensional NG sheets were well decorated by AgBr NPs with relative uniform dispersion, while pure AgBr NPs tended to aggregate and decompose (see ESI,† Fig. S2). It illustrated that the combination of AgBr NPs and the NG contributed to the stability of AgBr. As a result, it is expected that AgBr–NG nanocomposites would exhibit more excellent performances in applications compared with pure AgBr NPs.

Fig. 2A depicted the ECL curves of the AgBr–NG/GCE in the absence (curve a) and presence (curve b) of the coreactant $K_2S_2O_8$ by cycling the potential between 0.00 and −1.80 V. In the 0.10 M phosphate buffer solution (PBS) (pH = 8.0) containing 0.07 M $K_2S_2O_8$, the reduced potential obtained from the cyclic voltammetry (CV) (Fig. 2A, curve d) was at −0.65 V, corresponding to the reduction of $S_2O_8^{2-}$,[14] which did not appear when the AgBr–NG modified electrode was scanned in blank PBS (curve c). Moreover, an intense ECL emission was obtained at the AgBr–NG/GCE with 0.07 M $K_2S_2O_8$ and a very inconspicuous but cannot being ignored ECL signal was obtained without $K_2S_2O_8$, indicating that AgBr NPs acted as the luminophore and the coreactant $K_2S_2O_8$ may play a crucial role in the ECL process. There are two dominant pathways through which ECL can be generated, namely the annihilation and coreactant pathways.[1a] The electronic band gaps of AgBr NPs have been previously explored, and the edge positions of the conduction band and the valence band are −1.04 eV and −3.64 eV (*vs.* NHE), respectively.[15] So, it is energetically possible for electron transfer from the GCE to the conduction band of AgBr NPs if the applied potential on the working electrode is more negative than that of the conduction band of AgBr NPs shown in Scheme 1. To further investigate the ECL mechanism, we measured the ECL spectra of AgBr–NG nanocomposites by employing a series of optical filters (see ESI,† Fig. S3). The ECL emission band showed two emission maxima at 400 nm and 540 nm (Fig. S3B, ESI†), which was consistent with the PL peak in Fig. S3A (ESI†). This phenomenon implied that AgBr NPs were the luminescent species and the excited states obtained by electrochemical reactions were the same as those generated by photo-excitation,[6] which was similar to other semiconductors.[16] The two peaks of the ECL spectrum coinciding with the PL spectrum come from the transitions of different excited states to the ground state.[6,17]

The ECL behaviour of AgBr–NG–$K_2S_2O_8$ is similar to other systems, such as graphite-like carbon nitride and Ag_2Se

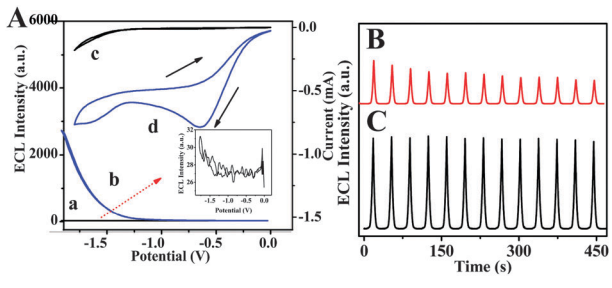

Fig. 2 (A) ECL-potential (a, b) and CV (c, d) curves of the AgBr–NG/GCE in 0.10 M PBS without (a, c) and with (b, d) 0.07 M $K_2S_2O_8$. The inset displays the enlarged view of curve a. Stability of ECL intensities from the (B) AgBr/GCE and (C) AgBr–NG/GCE.

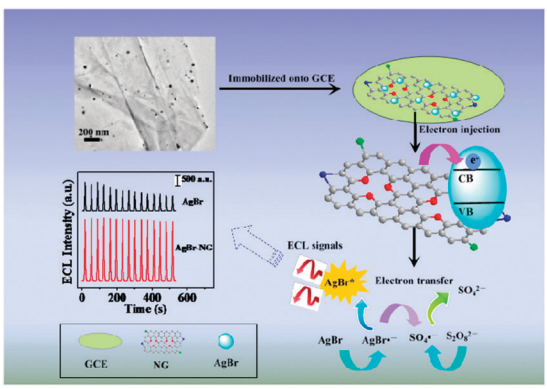

Scheme 1 Schematic illustration of the charge-transfer processes between the GCE and AgBr–NG and the ECL mechanism of AgBr–NG nanocomposites.

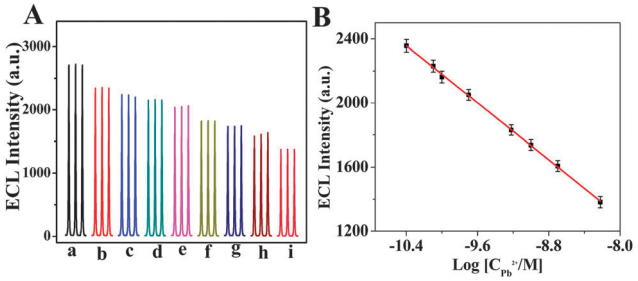

Fig. 3 (A) ECL intensity–time curve of the Pb^{2+} sensor with different Pb^{2+} concentrations. From (a) to (i): 0, 0.04, 0.08, 0.1, 0.2, 0.6, 1.0, 2.0 and 6.0 nM, respectively. (B) The calibration curve for Pb^{2+} determination. Error bars: ±SD n = 5.

quantum dots.[8,18] As the potential is negative enough, electrons are injected into the AgBr–NG nanocomposites and electrogenerated anion radicals ($AgBr^{\bullet -}$) are formed. Meanwhile, the reduction of $S_2O_8^{2-}$ releases a strong oxidizing agent, $SO_4^{\bullet -}$ radicals, which accept an electron from the anion $AgBr^{\bullet -}$ to form the AgBr* emitters for ECL emission. In this process, NG plays the role of accelerating the electron-transfer rate and the capacitance of electrons. Therefore, the mechanism of reaction is assumed as follows:

$$S_2O_8^{2-} + e^- \rightarrow S_2O_8^{\bullet 3-} \quad (1)$$

$$S_2O_8^{\bullet 3-} \rightarrow SO_4^{2-} + SO_4^{\bullet -} \quad (2)$$

$$AgBr + e^- \rightarrow AgBr^{\bullet -} \quad (3)$$

$$AgBr^{\bullet -} + SO_4^{\bullet -} \rightarrow AgBr^* + SO_4^{2-} \quad (4)$$

$$AgBr^* \rightarrow AgBr + h\nu \quad (5)$$

Furthermore, the very key point is that NG plays an important role in stabilizing the ECL intensity of AgBr NPs in our studies. From Fig. 2B, in the absence of NG, the ECL response of the AgBr/GCE rapidly degraded and was rather unstable, while the ECL signal of the AgBr–NG/GCE remained at an almost constant value during consecutive cyclic potential scanning (Fig. 2C), which might be attributed to the ECL passivation.[19] It illustrated that the combination of AgBr NPs and the NG contributed to the stability of AgBr NPs. One probable reason is that nitrogen-doped graphene functioned as an electron reservoir injected from the conduction band (CB) of n-type AgBr, avoiding the effect of the photogenerated electrons being captured by the Ag^+ in the process of ECL.[20] This result indicated that the ECL intensity of the AgBr–NG–$S_2O_8^{2-}$ system was highly repeatable over time due to the introduction of NG. Therefore, the system could serve as a sensing platform for the detection of analytes in our experiment. Besides, the ECL performances of AgBr–graphene oxide (GO) and AgBr–graphene sheets (GNs) were investigated in Fig. S4 (ESI†), which revealed that AgBr–NG was superior to that of AgBr–GO and AgBr–GNs.

In our work, it was found that the ECL emission of the AgBr–NG/GCE was effectively quenched by trace amounts of Pb^{2+}. To reduce the interference from the other ions, L-cysteine was added to the solution as a masking agent and the interference can be strongly improved as shown in Fig. S6B (ESI†), while it was still very sensitive to Pb^{2+}. Fig. 3A displayed the ECL intensities of the AgBr–NG/GCE in 0.07 M $K_2S_2O_8$ (pH = 8.0) at various concentrations of lead ions (0.0–6 nM). Under the optimal conditions (see ESI,† Fig. S5), the ECL intensity of the AgBr–NG/GCE showed a good linear relationship to logarithm of the molar concentration value of Pb^{2+} (Fig. 3B). The linear range was from 40 pM to 6 nM with a low detection limit of 1.3 pM (S/N = 3).

The selectivity of this sensing system was examined by testing several other interfering cations commonly coexisting with Pb^{2+} (such as Cr^{2+}, Ni^{2+}, Cd^{2+}, Zn^{2+}, Hg^{2+}, Ca^{2+}, Cu^{2+}, Al^{3+} and Co^{2+}) under identical conditions. As shown in Fig. S4 (ESI†), a remarkable ECL intensity decrease was obtained for Pb^{2+}, whereas no significant intensity changes were observed for the other metal ions. These results revealed that the approach is highly sensitive and selective toward Pb^{2+}.

In conclusions, we prepared AgBr–NG nanocomposites with a facile method and firstly observed the ECL emission from AgBr–NG nanocomposites and AgBr NPs. Compared to pure AgBr NPs, not only the stability of the AgBr NPs but also the intensity and stability of ECL emission from AgBr–NG nanocomposites were markedly improved. Then we successfully fabricated a simple and cost effective ECL sensor with this material for the detection of lead ions, demonstrating that it could be a novel class of efficient and promising luminophores for ECL sensing. It could open a new avenue in the preparation of stable and strong ECL nanocomposite films for analytical applications.

This work was supported by the National Natural Science Foundation of China (No. 21175061, 21375050 and 21405062), a Project Funded by the Priority Academic Program Development of Jiangsu Higher Education Institutions (No. PAPD-2014-37), Qing Lan Project and Key Laboratory of Modern Agriculture Equipment and Technology (No. NZ201109).

Notes and references

1 (*a*) M. M. Richter, *Chem. Rev.*, 2004, **104**, 3003; (*b*) L. Z. Hu and G. B. Xu, *Chem. Soc. Rev.*, 2010, **39**, 3275.
2 J. W. Oh, Y. O. Lee, T. H. Kim, K. C. Ko, J. Y. Lee, H. Kim and J. S. Kim, *Angew. Chem., Int. Ed.*, 2009, **48**, 2522.
3 S. N. Ding, J. J. Xu and H. Y. Chen, *Chem. Commun.*, 2006, 3631.
4 J. Li, Y. H. Xu, H. Wei, T. Huo and E. K. Wang, *Anal. Chem.*, 2007, **79**, 5439.
5 H. R. Zhang, J. J. Xu and H. Y. Chen, *Anal. Chem.*, 2013, **85**, 5321.
6 Y. M. Fang, J. Song, J. Li, Y. W. Wang, H. H. Yang, J. J. Sun and G. N. Chen, *Chem. Commun.*, 2011, **47**, 2369.
7 (*a*) G. Z. Zou, G. D. Liang and X. L. Zhang, *Chem. Commun.*, 2011, **47**, 10115; (*b*) L. Deng, Y. Shan, J. J. Xu and H. Y. Chen, *Nanoscale*, 2012, **4**, 831; (*c*) M. Han, Y. R. Li, H. Y. Niu, L. L. Liu, K. J. Chen, J. C. Bao, Z. H. Dai and J. M. Zhu, *Chem. – Eur. J.*, 2011, **17**, 3739.
8 C. M. Cheng, Y. Huang, X. Q. Tian, B. Z. Zheng, Y. Li, H. Y. Yuan, D. Xiao, S. P. Xie and M. M. F. Choi, *Anal. Chem.*, 2012, **84**, 4754.
9 (*a*) W. X. Wang, L. Q. Jing, Y. C. Qu, Y. B. Luan, H. G. Fu and Y. C. Xiao, *J. Hazard. Mater.*, 2012, **243**, 169; (*b*) P. Wang, B. Huang, X. Zhang, X. Qin, H. Jin, Y. Dai, Z. Wang, J. Wei, J. Zhan, S. Y. Wang, J. P. Wang and M. H. Whangbo, *Chem. – Eur. J.*, 2009, **15**, 1821.
10 Y. G. Xu, H. Xu, J. Yan, H. M. Li, L. Y. Huang, Q. Zhang, C. J. Huang and H. L. Wan, *Phys. Chem. Chem. Phys.*, 2013, **15**, 5821.

11 B. Cai, X. Y. Lv, S. Y. Gan, M. Zhou, W. G. Ma, T. S. Wu, F. H. Li, D. X. Han and L. Niu, *Nanoscale*, 2013, **5**, 1910.
12 (*a*) L. Xu, J. X. Xia, H. Xu, J. Qian, J. Yan, L. G. Wang, K. Wang and H. M. Li, *Analyst*, 2013, **138**, 6721; (*b*) J. Li, S. J. Guo and E. K. Wang, *RSC Adv.*, 2012, **2**, 3579.
13 (*a*) H. B. Wang, M. S. Xie, L. Thia, A. Fisher and X. Wang, *J. Phys. Chem. Lett.*, 2014, **5**, 119; (*b*) W. J. Lee, U. N. Maiti, J. M. Lee, J. Lim, T. H. Han and S. O. Kim, *Chem. Commun.*, 2014, **50**, 6818.
14 Y. T. Yan, Q. Liu, K. Wang, L. Jiang, X. W. Yang and J. Qian, *Analyst*, 2013, **138**, 7101.
15 (*a*) M. A. Asi, C. He, M. H. Su, D. H. Xia, L. Lin, H. Q. Deng, Y. Xiong, R. L. Qiu and X. Z. Li, *Catal. Today*, 2011, **175**, 256; (*b*) L. S. Zhang, K. H. Wong, Z. G. Chen, J. C. Yu, J. C. Zhao, C. Hu, C. Y. Chan and P. K. Wong, *Appl. Catal., A*, 2009, **363**, 221.
16 C. Z. Wang, Y. F. E, L. Z. Fan, Z. H. Wang, H. B. Liu, Y. L. Li, S. H. Yang and Y. L. Li, *Adv. Mater.*, 2007, **19**, 3677.
17 L. Zhang, Y. M. Fang, R. Y. Wang, L. X. You, N. Y. Fu, G. N. Chen and J. J. Sun, *Chem. Commun.*, 2011, **47**, 3855.
18 R. Cui, Y. P. Gu, L. Bao, J. Y. Zhao, B. P. Qi, Z. L. Zhang, Z. X. Xie and D. W. Pang, *Anal. Chem.*, 2012, **84**, 8932.
19 (*a*) L. C. Chen, X. T. Zeng, P. Si, Y. M. Chen, Y. W. Chi, D. H. Kim and G. N. Chen, *Anal. Chem.*, 2014, **86**, 4188; (*b*) R. E. Palacios, F. R. Fan, J. K. Grey, J. Suk, A. J. Bard and P. F. Barbara, *Nat. Mater.*, 2007, **16**, 680.
20 (*a*) B. Cai, X. Y. Lv, S. Y. Gan, M. Zhou, W. G. Ma, T. S. Wu, F. H. Li, D. X. Han and L. Niu, *Nanoscale*, 2013, **5**, 1910; (*b*) C. Dong, K. L. Wu, X. W. Wei, J. Wang, L. Liu and B. B. Jiang, *Appl. Catal., A*, 2014, **488**, 11.

